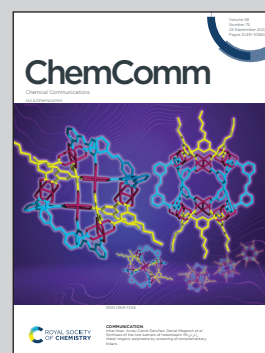


Showcasing research from Professor Furuta's laboratory,
Department of Biomolecular Science, Toho University,
Chiba, Japan

Elucidation of the working principle of a gene-directed
caged HDAC inhibitor with cell-type selectivity

The concept of a gene-directed caging strategy has been
applied to prepare a doubly "locked" prodrug that can
genetically target cells of interest. This work demonstrates
photochemical regulation of endogenous histone deacetylase
activity in mammalian cells.

As featured in:



See Toshiaki Furuta *et al.*,
Chem. Commun., 2022, **58**, 10484.



 Cite this: *Chem. Commun.*, 2022, 58, 10484

 Received 27th June 2022,
 Accepted 18th August 2022

DOI: 10.1039/d2cc03552a

rsc.li/chemcomm

Elucidation of the working principle of a gene-directed caged HDAC inhibitor with cell-type selectivity†

 Kotoko Sakamoto, Ayumi Hirano, Rika Hidaka, Akinobu Z. Suzuki, Taro Ueno 
 and Toshiaki Furuta *

Histone deacetylases (HDACs) play crucial roles in the epigenetic regulation of gene expression. Here, we report CM-Bhc-SAHA, a novel caged HDAC inhibitor, genetically targeting cells of interest. Mammalian cells expressing porcine liver esterase led to the optochemical inhibition of endogenous HDAC activity when treated with CM-Bhc-SAHA and irradiated with 405 nm light.

Epigenetic regulation of gene expression critically regulates physiological processes such as proliferation,¹ development,² and cellular memory³ and potentially causes common diseases such as cancer.⁴ Histone acetylation is a primary epigenetic process that regulates transcription by loosening or tightening chromatin structure. Histone deacetylases (HDACs) are enzymes that catalyze the deacetylation of *ε*-acetylated lysine residues and mainly promote repression of gene expression.^{5,6} There are two types of HDAC families:⁷ Zinc-dependent Class I (HDAC 1–3, 8), IIa (HDAC 4–7, 9), IIb (HDAC 6, 10), IV (HDAC 11), and NAD-dependent Class III (SIRT1–7). Recent studies have shown that many non-histone target proteins are dynamically deacetylated by HDACs outside the nucleus, thereby demonstrating HDAC functions beyond the chromatin.⁸ HDAC dysregulation causes various diseases: abnormal expression of Class I HDACs in broad ranges of cancer cells,⁹ an association of deregulation of Class I (HDAC 1 and 2) and Class IIb (HDAC6) with cognitive impairment,¹⁰ and neurodegenerative diseases.¹¹ Thus, HDAC inhibitors (HDACi) have emerged as chemical probes to elucidate post-transcriptional protein modification mechanisms and as drug candidates for treating diseases such as cancer¹² and neurodegenerative disorders.¹³ The pan-selective nature of the HDACi for the HDAC family would render off-target effects upon systemic administration.

Tissue- and cell-type-selective modulation of HDAC activity is desirable for basic research and clinical applications. To achieve this goal, light-controlled modulation of HDAC activity by photo-responsive chemical probes, such as azobenzene-derived reversible HDAC inhibitors^{14,15} and photocaged HDACi,^{16–20} has been reported. Light triggering of photocaged compounds is a powerful technique that can control biological systems with high spatiotemporal resolution in experimental designs with adherent cells or tissue slices.^{21–23} Caged compounds are small molecular weight organic compounds that are not genetically encoded, and hence cannot target specific types of cells or tissues of interest. To overcome this problem, we recently reported the concept of gene-directed caged compounds that are photoactivated only in cells tagged with preselected genes.²⁴ Our gene-directed caging strategy allows the use of a variety of substrate/enzyme pairs as photochemical “locks” and their “key” enzymes. In our previous paper, we used a pair of β -galactosyl moiety and *E. coli* β -galactosidase to prepare gene-directed caged cyclic nucleotides that function as optochemical tools with cell-type selectivity.²⁴ This study reports a new gene-directed caged HDAC inhibitor with the 1-methyl-1-cyclopropanecarboxylmethyl (CM) moiety as a chemical lock to expand the repertoire of gene-directed caged compounds and achieve cell-type selective inhibition of HDAC activity. The CM group was designed to be orthogonally hydrolyzed in mammalian cells only in the presence of externally expressed porcine liver esterase (PLE).²⁵

For our proof-of-concept experiments, as an HDACi, we chose suberoylanilide hydroxamic acid (SAHA), also known as vorinostat, a pan-selective HDAC inhibitor effective in both Classes I and IIb HDACs.²⁶ This hydroxamic acid coordinates to zinc ions, located inside the active site of HDAC. Therefore, we decided to mask this group with a CM-Bhc group to suppress its inhibitory activity. We hypothesized the locked caged HDAC inhibitor CM-Bhc-SAHA to be photoactivatable only in the presence of its “key” enzyme PLE (Fig. 1).

Synthesis of Bhc-caged SAHAs was performed starting from MOMBhc-CH₂OH,²⁷ as shown in Scheme 1. The 4-hydroxymethyl

Department of Biomolecular Science, Faculty of Science, Toho University, 2-2-1 Miyama, Funabashi, 274-8510, Japan. E-mail: furuta@biomol.sci.toho-u.ac.jp

† Electronic supplementary information (ESI) available. See DOI: <https://doi.org/10.1039/d2cc03552a>



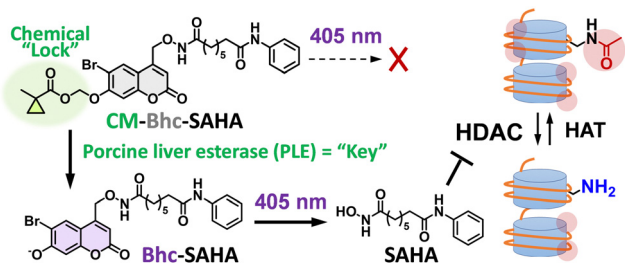


Fig. 1 Gene-directed caged HDAC inhibitor. CM-Bhc-SAHA is inert to 405 nm light because of a chemical “lock” on it. The lock is removed by its “key” enzyme, PLE, to produce Bhc-SAHA, which can release an HDAC inhibitor SAHA when exposed to 405 nm light.

group was converted to alkoxyamine by Mitsunobu reaction and reduction²⁸ to yield **MOMBhc-CH₂ONH₂** (**1**). Esterification with suberanilic acid and removal of MOM protection produced **Bhc-SAHA** (**2**). Alkylation of the 7-OH group with CM moiety yielded a candidate for gene-directed caged SAHA, **CM-Bhc-SAHA** (**3**). This synthetic method can also be applied to other HDAC inhibitors with hydroxamic acids, such as Trichostatin A and Panobinostat.

The absorption maximum of **3** is at 330 nm in an aqueous solution at neutral pH, while that of **2** is at 374 nm. **CM-Bhc-SAHA** does not absorb light at a wavelength longer than 380 nm (purple shaded area in Fig. 2a). Therefore, we hypothesized 405 nm light irradiation to cause selective uncaging of **2** in the presence of **3**. The time course of photolysis of caged SAHAs is shown in Fig. 2b where **Bhc-SAHA** produced SAHA (Fig. S1, ESI[†]) at 405 nm (3.4 mJ s^{-1}) with a photolysis quantum yield (Φ_{405}) of 0.12. Photolysis efficiency ($\epsilon\Phi$) of $900 \text{ M}^{-1} \text{ cm}^{-1}$ is higher than that of previously reported diethylaminocoumarin-caged SAHA¹⁶ and lower than that of Bhc-cAMP ($\epsilon\Phi$ $2840 \text{ M}^{-1} \text{ cm}^{-1}$).²⁴ The difference in quantum yield observed between Bhc-SAHA (0.12) and Bhc-cAMP (0.40) can be attributed to changes related to the difference in the acidity of the leaving groups. The pK_a of the hydroxamic acid moiety of SAHA is 9.2, which is much more weakly acidic than that of the cyclic phosphate of cAMP (pK_a 3.92). As expected from its absorption properties, no photolytic

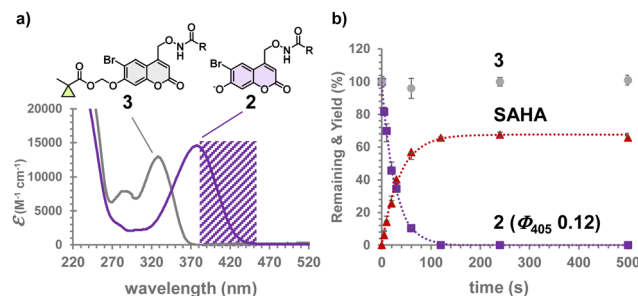
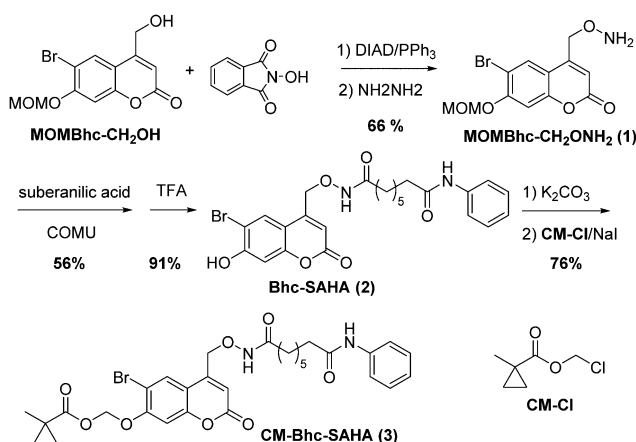


Fig. 2 Photolysis of caged cNMPs. (a) UV-vis absorption spectra of caged SAHAs in an aqueous solution (pH 7.4). Most of the phenolic OH of **2** is ionized in this condition. (b) Photolysis time course of the caged SAHAs. Samples ($10 \mu\text{M}$) were irradiated at 405 nm (3.4 mJ s^{-1}) under simulated physiological conditions (pH 7.4). **2** (purple square), SAHA released from **2** (red triangle), **3** (gray circle). The dashed lines are the best fit for single exponential decay and rise. The values represent the averages of triplicate experiments \pm the standard deviation (SD) of the mean.

consumption of **3** was observed under the same irradiation conditions, confirming that the modification by the CM group locks the photolability of **3** (Fig. 2b).

The hydrolytic stability of caged SAHA was measured in an aqueous solution at neutral pH under dark conditions; no traceable amounts of degradation were observed after 15 days for **2** and 5 days for **3**. Because SAHA is hydrolysed in the presence of plasma proteins (half-life 75–115 min),²⁹ degradation of **3** was observed in serum containing medium at $37 \text{ }^\circ\text{C}$. Since only 4% conversion from **3** to **2** was observed after 24 h, stability was not considered to be a problem in subsequent experiments.

We checked whether locked caged SAHA **3** served as a substrate of PLE and produced unlocked **2** with a practically usable reactivity. Thus, we treated **3** with PLE from the porcine liver. Analysis of the reaction mixture by HPLC confirmed the yield of **2** to be 80% (Fig. 3a and Fig. S2, ESI[†]). The Michaelis constant (K_m) and apparent reaction rate (k_{cat}) of **3** were $3.2 \mu\text{M}$ and 0.87 s^{-1} , respectively. The specificity constant (k_{cat}/K_m) was determined to be $2.7 \times 10^5 \text{ M}^{-1} \text{ s}^{-1}$, comparable to reported CM derivatives, such as fluorescein-CM₂ ($K_m = 0.50 \mu\text{M}$, $k_{\text{cat}}/K_m = 5.1 \times 10^4 \text{ M}^{-1} \text{ s}^{-1}$).²⁵ The results indicated that **3** is a



Scheme 1 Synthesis of CM-Bhc-SAHA.

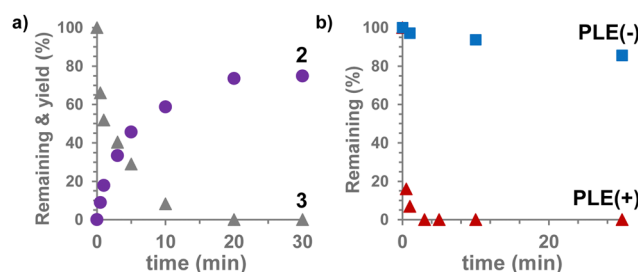


Fig. 3 Enzymatic transformation of **CM-Bhc-SAHA** (**3**) with PLE. (a) $5.4 \mu\text{M}$ of **3** was treated with $1.5 \times 10^{-2} \text{ U mL}^{-1}$ of PLE (from the porcine liver). The remaining percentage of **3** (gray triangle) and formation of **Bhc-SAHA** (**2**) (purple circle). (b) Time course for the enzymatic transformation of **3** with HEK293T cell lysates. PLE(+) lysates: red triangle, PLE(-) lysates: blue square.



suitable substrate for PLE and produces **2** with a reactivity comparable to known substrates that have been successfully used in live-cell experiments.

Next, we examined the effect of mammalian internal esterases on the hydrolytic stability of the 1-methylcyclopropylcarboxy methyl group (CM). Therefore, **3** was treated with either HEK293T/PLE (PLE(+)), which constitutively expresses the PLE gene, or HEK293T (PLE(-)), which does not express PLE. The conversion from **3** to **2** was completed in 1 minute, using PLE(+) cell lysate, suggesting the practical reactivity of **3** for PLE expressed in mammalian cultured cells (Fig. 3b and Fig. S3, ESI[†]). Unexpectedly, the PLE(-) lysate gradually deprotected the CM group under the same reaction conditions (15% conversion in 30 min). Since **3** was hydrolytically stable at neutral pH during the experiments, the deprotection observed with PLE(-) lysates was considered a consequence of enzymatic hydrolysis catalyzed by internal esterases. To confirm that SAHA is photochemically produced from **3** in the presence of PLE(+) cells, the reaction mixtures were irradiated with 405 nm light; **3** was incubated with PLE(+) or PLE(-) cell lysates for 1 h and irradiated with 405 nm light (3.4 mJ s^{-1}) for 120 s. HPLC analysis revealed that SAHA was produced only from PLE(+) lysate (Fig. S4, trace 2, ESI[†]) and not from the PLE(-) one (Fig. S4, trace 4, ESI[†]).

In HEK293T cells, the internal esterase-mediated enzymatic hydrolysis of the CM moiety of **3** was not entirely suppressed, although, the reactivity with PLE was much better than that with internal esterases in the test cells, suggesting **3** can be used as a gene-directed caged SAHA with PLE as a “key” enzyme.

The introduction of caging groups must inhibit the HDAC inhibitory activity of caged SAHAs. Therefore, we measured the lysine deacetylation activity of HDACs from HeLa cell nuclear extracts in the presence of caged SAHAs (Fig. 4a). The half-maximal inhibitory concentrations (IC_{50}) of caged SAHAs were $16.2 \mu\text{M}$ for **2** and over $70 \mu\text{M}$ for **3**, which was $1/1000$ of the inhibitory activity of unmodified SAHA ($IC_{50} 39.6 \text{ nM}$). Since SAHA is a nonspecific, broad-spectrum inhibitor of HDAC subtypes²⁶ and Class I HDACs primarily involve HeLa cell nuclear extracts, the IC_{50} values observed with caged SAHAs must directly reflect the suppression of inhibitory activity achieved by the caging of hydroxamate moiety. The lesser residual activity of CM-Bhc, which is bulkier than Bhc, is also consistent with the caging effect. The bulkiness of the chemical lock allows caged SAHAs to suppress residual HDACi activity in non-target cells and, as a result, suppress the undesirable off-target effects.

Since the CM-Bhc caging group is converted to Bhc group when applied to PLE-expressing cells, we examined photo-induced HDAC inhibition both in a cuvette and in cells using **2**. HDAC activity was quantified after incubation of HeLa cell nuclear extracts with 500 nM of **2** and irradiation with 405 nm light (3.4 mJ s^{-1}). As shown in Fig. S5 (ESI[†]), photon dose-dependent inhibition of HDAC activity was observed in the presence of **2**, confirming that photochemically liberated SAHA achieved HDAC inhibition.

The compounds were then tested in live cultured cells. SAHA was added to live HEK293T cells to estimate the working

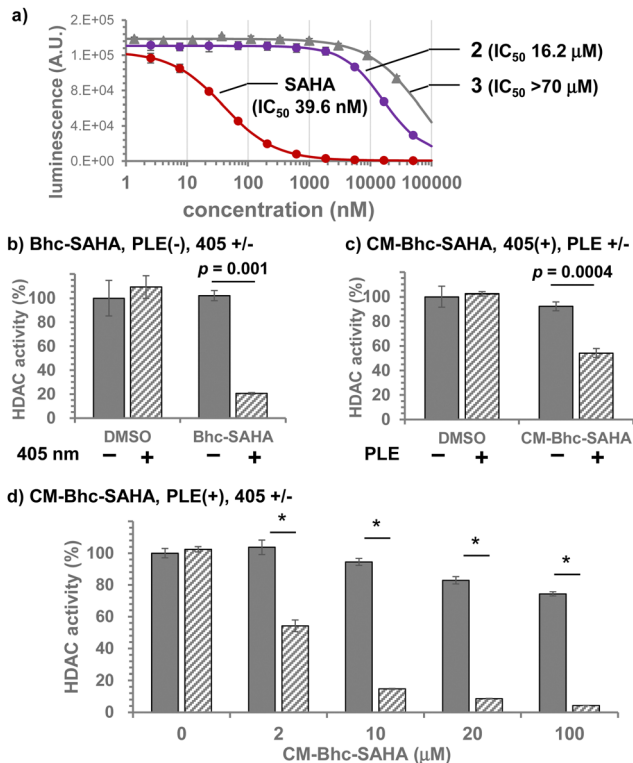


Fig. 4 Inhibition of HDAC activity in-cuvette and in-cell experiments. (a) Inhibition of HDAC in HeLa nuclear extracts. Enzymatic activity of HeLa HDACs was measured in the presence of the tested compounds: SAHA (red circle), **2** (purple circle), and **3** (gray triangle). Solid lines are best fitted to the nonlinear regression model. (b)–(d) Photo-mediated inhibition of endogenous HDAC in HEK293T cells. Cells were treated with the indicated compounds for 1 h. The cells were washed with PBS to remove the compound in the culture media and irradiated at 405 nm (3.4 mJ s^{-1}) for 60 s. The enzymatic activity of HDACs from non-irradiated control cells treated with DMSO alone was quantified. Percentages of the HDAC activity were normalized to this group. The values represent the averages of triplicate experiments \pm the standard deviation (SD) of the mean. (b) Effect of 405 nm irradiation. Cells were treated with $100 \mu\text{M}$ of **2**. Solid gray: non-irradiated, Shaded light gray: irradiated. (c) Effect of PLE expression. Cells were treated with $2 \mu\text{M}$ of **3**. Solid gray: PLE(-), Shaded light gray: PLE(+). (d) Dose dependency. PLE(+) cells were treated with the indicated concentration of **3** and then exposed to 405 nm light. Solid gray: non-irradiated, Shaded light gray: irradiated. * Student's *T*-test $p < 0.0005$.

concentration, and the deacetylation activity of endogenous HDACs was quantified (Fig. S6, ESI[†]). 625 nM SAHA in culture medium achieved approximately 40% inhibition. This HDACi activity was consistent with the in-cuvette experiments shown in Fig. S5 (ESI[†]), in which 500 nM Bhc-SAHA caused 52% HDAC inhibition when exposed to 405 nm light (204 mJ cm^{-2} , relative HDAC activity: DMSO 71.6%, Bhc-SAHA 37.6%). Since the expected concentration of photochemically released intracellular SAHA was likely lower than the caged SAHAs applied to the culture media, subsequent experiments were performed using caged compounds at concentrations of $2 \mu\text{M}$ or higher.

Incubation of HEK293T cells with $100 \mu\text{M}$ of **2** and irradiation with 405 nm light (204 mJ cm^{-2}) inhibited approximately 80% of endogenous HDAC activity. Under these conditions,



neither 405 nm light irradiation nor adding **2** alone affected the endogenous HDAC activity (Fig. 4b). When the effect of PLE expression was tested in HEK293T (PLE(-)) or HEK293T/PLE (PLE(+)) cells using 2 μM of **3**, HDAC activity was inhibited by 40% only when PLE(+) cells were exposed to 405 nm light (Fig. 4c). Fig. 4d shows the dose dependence of HDACi activity of **3** when exposed to 405 nm light (204 mJ cm^{-2}), confirming that the majority of endogenous HDAC activity in PLE(+) cells is almost completely suppressed photochemically by the addition of 10 μM or more of **3** to the culture media. From these results, we conclude that **CM-Bhc-SAHA (3)** is a membrane-permeable gene-directed caged SAHA that can selectively suppress endogenous HDAC activity in cells expressing the “key” enzyme, PLE.

In conclusion, we developed a new caged HDAC inhibitor that can genetically target cells of interest. **CM-Bhc-SAHA (3)** is stable in an aqueous solution at neutral pH, is inert to 405 nm irradiation, and produces **Bhc-SAHA (2)** with practical reactivity ($k_{\text{cat}}/K_{\text{m}} 2.7 \times 10^5 \text{ M}^{-1} \text{ s}^{-1}$) as a substrate for PLE. The HDAC inhibitory activities of caged SAHAs **2** and **3** were suppressed by a factor of 10^3 compared to SAHA alone. The target cells were tagged with an externally expressed PLE gene, and photo-induced selective inhibition of endogenous HDAC activity was achieved using a new caged SAHA **3**. Thus, the CM-Bhc group is a new addition to the gene-directed photocaging groups that can be selectively uncaged by 405 nm light irradiation in the presence of its “key” enzyme. The same gene-directed caging strategy can be applied to other class-selective HDAC inhibitors having hydroxamic acid moieties.³⁰ Gene-directed caged HDAC inhibitors would further expand the utility of methods to modulate HDACi activity in a cell- and tissue-type-selective and spatiotemporal manner. Some issues remain to be improved. Uncaging by PLE and 405 nm light should only occur in cells expressing PLE, but since the Bhc-SAHA and SAHA produced are membrane permeable, they could diffuse out of the cells and re-enter nearby cells, reducing cell type selectivity. This can be an inherent drawback of this system as long as a membrane-permeable HDACi is used.

By utilizing the concept of gene-directed caging, cell-type targetability can be incorporated into previously reported Bhc-caged compounds.^{31,32} Furthermore, because of their substrate specificity, it is possible to use two or more chemical lock-and-key enzyme pairs in a biologically orthogonal manner. This would allow, for example, the simultaneous targeting of two or more caged molecules and separate targeting of different types of cells or tissues.

This work was supported by JSPS KAKENHI grant number 20H02882 (TF) and a Grant-in-Aid for Scientific Research on Innovative Areas 19H05778 (TF) “MolMovies.” We thank Ms Sayaka Kado (Chiba University) for the measurement of HR-MS.

Conflicts of interest

There are no conflicts to declare.

Notes and references

- 1 N. Reichert, M.-A. Choukallah and P. Matthias, *Cell. Mol. Life Sci.*, 2012, **69**, 2173–2187.
- 2 J. C. Kiefer, *Dev. Dyn.*, 2007, **236**, 1144–1156.
- 3 R. M. Barrett and M. A. Wood, *Learn. Mem.*, 2008, **15**, 460–467.
- 4 M. Esteller, *N. Engl. J. Med.*, 2008, **358**, 1148–1159.
- 5 A. J. M. d Ruijter, A. H. v Gennip, H. N. Caron, S. Kemp and A. B. P. v Kuilenburg, *Biochem. J.*, 2003, **370**, 737–749.
- 6 E. Seto and M. Yoshida, *Cold Spring Harbor Perspect. Biol.*, 2014, **6**, a018713–a018713.
- 7 S.-Y. Park and J.-S. Kim, *Exp. Mol. Med.*, 2020, **52**, 204–212.
- 8 I. Ali, R. J. Conrad, E. Verdin and M. Ott, *Chem. Rev.*, 2018, **118**, 1216–1252.
- 9 B. Barneda-Zahonero and M. Parra, *Mol. Oncol.*, 2012, **6**, 579–589.
- 10 P.-C. Pao and L.-H. Tsai, *ACS Chem. Neurosci.*, 2022, **13**, 848–858.
- 11 M. Lemos and N. Stefanova, *Front. Synaptic Neurosci.*, 2020, **12**, 586453.
- 12 Y. Lu, Y.-T. Chan, H.-Y. Tan, S. Li, N. Wang and Y. Feng, *Mol. Cancer*, 2020, **19**, 79.
- 13 A. M. Burns and J. Gräff, *Curr. Opin. Neurobiol.*, 2021, **67**, 75–84.
- 14 S. A. Reis, B. Ghosh, J. A. Hendricks, D. M. Szantai-Kis, L. Tork, K. N. Ross, J. Lamb, W. Read-Button, B. Zheng, H. Wang, C. Salthouse, S. J. Haggarty and R. Mazitschek, *Nat. Chem. Biol.*, 2016, **12**, 317–323.
- 15 W. Szymanski, M. E. Ourailidou, W. A. Velema, F. J. Dekker and B. L. Feringa, *Chem. – Eur. J.*, 2015, **21**, 16517–16524.
- 16 N. Ieda, S. Yamada, M. Kawaguchi, N. Miyata and H. Nakagawa, *Bioorg. Med. Chem.*, 2016, **24**, 2789–2793.
- 17 A. Leonidova, C. Mari, C. Aebbersold and G. Gasser, *Organometallics*, 2016, **35**, 851–854.
- 18 B. Parasar and P. V. Chang, *Chem. Sci.*, 2017, **8**, 1450–1453.
- 19 L. L. Shi, L. Xu, Q. H. Guan, X. Jin, J. P. Yang and X. Y. Zhu, *Bioconjugate Chem.*, 2018, **29**, 1344–1351.
- 20 G. R. Sama, H. Liu, S. Mountford, P. Thompson, A. Robinson and A. E. Dear, *Bioorg. Med. Chem. Lett.*, 2020, **30**, 127291.
- 21 P. Klan, T. Solomek, C. G. Bochet, A. Blanc, R. Givens, M. Rubina, V. Popik, A. Kostikov and J. Wirz, *Chem. Rev.*, 2013, **113**, 119–191.
- 22 R. Weinstain, T. Slanina, D. Kand and P. Klán, *Chem. Rev.*, 2020, **120**, 13135–13272.
- 23 Y. Hou, Z. Zhou, K. Huang, H. Yang and G. Han, *ChemPhotoChem*, 2018, **2**, 1005–1011.
- 24 A. Z. Suzuki, T. Sakano, H. Sasaki, R. Watahiki, M. Sone, K. Horikawa and T. Furuta, *Chem. Commun.*, 2021, **57**, 5630–5633.
- 25 L. Tian, Y. L. Yang, L. M. Wysocki, A. C. Arnold, A. Hu, B. Ravichandran, S. M. Sternson, L. L. Looger and L. D. Lavis, *Proc. Natl. Acad. Sci. U. S. A.*, 2012, **109**, 4756–4761.
- 26 W. K. Kelly and P. A. Marks, *Nat. Clin. Pract. Oncol.*, 2005, **2**, 150.
- 27 A. Z. Suzuki, T. Watanabe, M. Kawamoto, K. Nishiyama, H. Yamashita, M. Ishii, M. Iwamura and T. Furuta, *Org. Lett.*, 2003, **5**, 4867–4870.
- 28 E. Grochowski and J. Jureczak, *Synth. Stuttgart*, 1976, 682–684.
- 29 R. Konsoula and M. Jung, *Int. J. Pharm.*, 2008, **361**, 19–25.
- 30 A. V. Bieliauskas and M. K. H. Pflum, *Chem. Soc. Rev.*, 2008, **37**, 1402–1413.
- 31 T. Furuta, S. S. H. Wang, J. L. Dantzker, T. M. Dore, W. J. Bybee, E. M. Callaway, W. Denk and R. Y. Tsien, *Proc. Natl. Acad. Sci. U. S. A.*, 1999, **96**, 1193–1200.
- 32 A. Z. Suzuki, R. Sekine, S. Takeda, R. Aikawa, Y. Shiraishi, T. Hamaguchi, H. Okuno, H. Tamamura and T. Furuta, *Chem. Commun.*, 2019, **55**, 451–454.

